CrystEngComm

Accepted Manuscript

ROYAL SOCIETY OF CHEMISTRY

www.rsc.org/crystengcomm

Crystallization and Characterization of Cocrystals of Piroxicam and 2,5-Dihydroxybenzoic Acid

E. M. Horstman,[a] J.A. Bertke,[b] E. H. Kim,[a] L. C. Gonzalez,[a] G. G. Z. Zhang,[c] Y. Gong,[c*] and P. J. A. Kenis [a]

Abstract. A cocrystal of piroxicam (PRX) and 2,5-dihydroxybenzoic acid (HBA), **PRX-HBA**, and an acetone (ACT) solvate of the cocrystal, **PRX-HBA-ACT**, were crystallized on a microfluidic platform *via* solvent evaporation. The inclusion of ACT was found serendipitously, with the ACT probably being introduced into the crystallization system as an impurity in HBA. The crystal structures of PRX-HBA and PRX-HBA-ACT obtained by X-ray diffraction both exhibit the $P2_1/c$ space group. Bulk quantities of the cocrystals were synthesized using a slurry method and their physical properties were characterized with thermogravimetric analysis and differential scanning calorimetry. Additionally, the phase behavior of PRX-HBA-ACT during desolvation was monitored with powder X-ray diffraction. The powder diffraction of PRX-HBA-ACT after complete desolvation has the same peak positions as the PRX-HBA, suggesting that PRX-HBA-ACT re-arranges to the structure of PRX-HBA.

Keywords: cocrystal; solvate; microfluidics; cocrystal screen; X-ray diffraction

Introduction

In the pharmaceutical industry BCS Class II drugs are reported to make up about 60-70% of drugs in the pipeline. These drugs are characterized by low solubility across physiological pH range.[1, 2] Crystallization of these pharmaceutical agents with cocrystal formers (CCFs) provides a way to enhance the physiochemical properties of the solid form[3-6] and improve their performance.[4, 5, 7] Thousands of food ingredients and additives have been recognized by the U.S. Food and Drug Administration as being safe for human consumption and a majority of this list may be acceptable for crystal engineering of pharmaceutical solids.[8] Since predictive cocrystal formation has not been fully developed, high throughput cocrystal screens with a large number of CCFs are often used to discover novel solid forms of a pharmaceutical agent. Many techniques have been developed for cocrystal screening including solution based (e.g. evaporation) and mechanochemical based (*e.g.*, grinding) approaches.[9]

Although high throughput cocrystal screens can be effective at generating novel cocrystals, the success of finding a cocrystal often depends on the screening method chosen.[10] Deeper understanding of cocrystal formation is needed to aid the more rational design of cocrystal screening experiments. For example, MacGillivray *et al.* has examined cocrystals of theophylline and caffeine to characterize intermolecular and intramolecular synthons.[9, 11, 12] This work also provided a systematic study to determine synthon hierarchies in molecules with multiple potential hydrogen bonding sites. Additionally, researchers at times analyze the several hundred thousand crystal structures of organic compounds available in the Cambridge Crystal Structure Database (CCSD), to help predict possible new co-crystals between CCFs and target APIs, based on hydrogen bond lengths and angles observed in previously reported structures.[13] Despite these efforts, current design of cocrystal screens typically incorporates minimal rational input, resulting in low success rates in most current cocrystal screening efforts.

Developing a deeper understanding of cocrystallization also relies on the ability to obtain the structure of the solid forms obtained in a cocrystal screen. Many cocrystal screens, however, do not result in the formation of diffraction quality crystals. In those cases, bulk characterization methods such as powder X-ray diffraction (PXRD) or Raman spectroscopy are used to differentiate among starting materials, cocrystals, and cocrystal polymorphs. Knowing the crystal structure of the cocrystal is the only way to unequivocally identify what solid form has been crystallized. In the case of AMG 517, the API surprisingly cocrystallized with sorbic acid (present in only trace quantities) in the final formulation.[14] This incident highlights the challenges in predicting solid formation.

Several microfluidic approaches have been investigated as a way to study formation of pharmaceutical solid forms, enabling the screening of more conditions with small amounts of material.[15-21] For example, in prior work we have demonstrated the use of microfluidic platforms to screen for cocrystals by diffusional mixing of an API solution and a CCF solution in adjacent compartments,[15] at times in combination with solvent evaporation.[22]

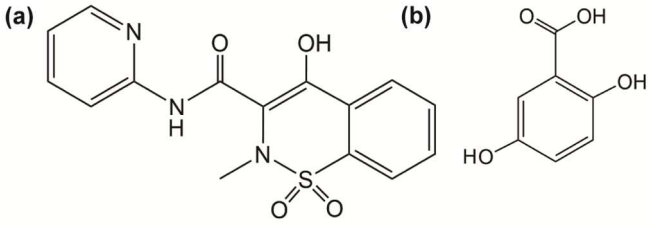

Figure 1. Chemical structures of (a) piroxicam and (b) 2,5-dihydroxybenzoic acid.

Here we investigate cocrystals of piroxicam (**PRX**) and 2,5-dihydroxybenzoic acid (**HBA**), Figure 1. PRX is a non-steroidal anti-inflammatory Class II drug. Three cocrystals of PRX and HBA have been previously reported.[10] All three solid forms were obtained by solution mediated phase transformation and characterized *via* Raman spectroscopy and PXRD. In this work, a simple microfluidic platform consisting of arrays of single wells was used to screen for solid forms of PRX and HBA and identify crystallization conditions to grow diffraction quality crystals. This platform simulates the experimental conditions of a 96 well platform, while utilizing less volume of sample per condition screened and providing more control over the rate of solvent evaporation. We discovered several interesting solid forms of PRX and HBA, one being a cocrystal that has not been reported and another being a cocrystal that incorporates an impurity into its structure forming a solvated cocrystal. The aforementioned solid forms were characterized further *via* thermogravimetric analysis (TGA), powder X-ray diffraction (PXRD), and differential scanning calorimetry (DSC).

Experimental

Platform Design and Fabrication

The crystallization platform used in this study is composed of a 6 x 6 micro-well array and one set of valves to allow fluidic routing, Figure 2. Each micro well is about 1250 µm x 1500 µm x 60 µm and houses approximately 110 nL of solution. The platform fabrication is detailed in previous work and is included in the Supplemental Information.[15, 22] Briefly, the platform is comprised of a thin poly-dimethylsiloxane (PDMS, General Electric RTV 615, Part A/B) control layer to control fluid routing and

a fluid layer to provide fluid storage. The PDMS layers are sandwiched between a cyclic olefin copolymer (COC, 6013 grade, TOPASTM Advanced Polymers) support layer and a substrate layer both provide physical rigidity and reduced solvent loss. The support, control, and fluid layers were irreversibly bound together, then this assembly was reversibly bound to the substrate layer to allow for easy access to the solids crystallized on-chip by peeling apart the chip, Figure 2.

Crystallization experiments

Materials. PRX (≥98.0%), HBA (≥98.0%), and 2,2,2-trifluoroethanol (≥99.0%) were purchased from Sigma-Aldrich (St. Louis, MO, USA) and were used as purchased. Acetonitrile (≥99.9%) was purchased from Fisher Scientific (Fair Lawn, NJ, USA) and methanol (≥99.9%) was purchased from EDM Chemical (Gibbstown, NJ, USA). Acetonitrile and methanol were used as purchased.

Single Crystal Growth. Single crystals of the PRX and HBA cocrystal (**PRX-HBA**) were grown on-chip from an acetonitrile solution. PRX was added to acetonitrile until saturation (~0.034M), and then an equimolar ratio of HBA was added to form a crystallization solution. The PRX and HBA crystallization solution was introduced on-chip. After filling, the chip was placed inside a Petri dish and sealed with Parafilm. After complete solvent evaporation (1 day), PRX-HBA crystals were observed on-chip. Initially the single crystal was characterized using on-chip Raman spectroscopy; then, a crystal was harvested from the chip for structure determination using single X-ray diffraction spectrometry.

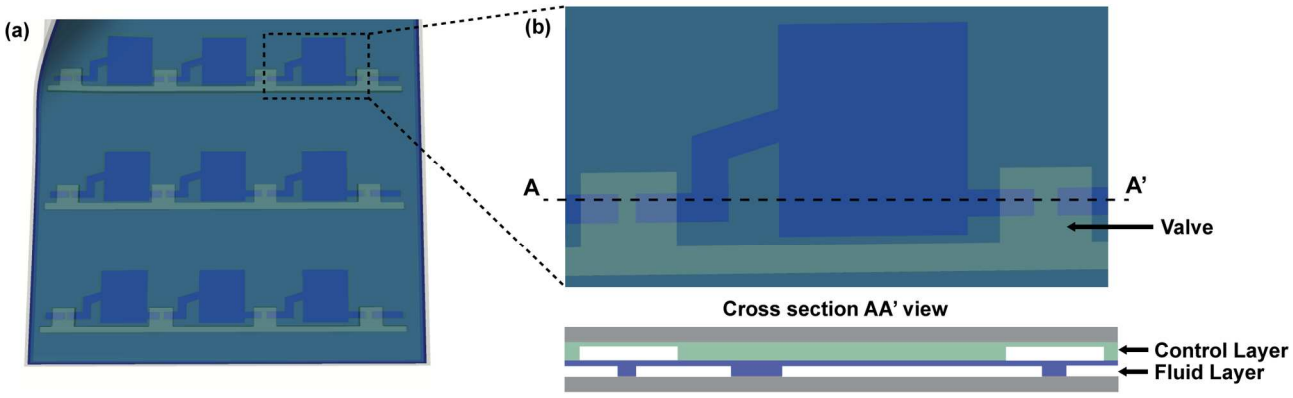

Figure 2. (a) A 3x3 array of the microfluidic platform showing that the platform can be peeled apart to harvest crystals grown on-chip. (b) Magnified view of a single well as well as a cross sectional view of the chip to highlight the position of the valves, and the 'zig-zag' design used to decrease trapping of bubbles when filling the chip.

Single crystals of PRX, HBA, and acetone (**PRX-HBA-ACT**) were grown on-chip from an acetonitrile solution. PRX was added to acetonitrile until saturation (~0.034M), then a 1.5 molar ratio of HBA was added to form a crystallization solution. The PRX and HBA crystallization solution was

introduced on-chip. After filling, the chip was placed inside a Petri dish and sealed with Parafilm. After complete solvent evaporation (1 day), the PRX-HBA-ACT crystals were observed on-chip. Initially the solid form was characterized with on-chip Raman spectroscopy. Since the Raman spectra matched with previously reported spectra[10] and the solids had good quality; a crystal was harvested from the chip for structure determination.

Bulk Crystallization. To crystallize greater quantities of the PRX-HBA cocrystal for further characterization, equimolar ratios of PRX and HBA were slurried in acetonitrile for 12 hours. The slurry was then filtered to isolate the solids and the solids were allowed to dry. Bulk PRX-HBA-ACT cocrystal was crystallized by slurrying equimolar ratios of PRX and HBA in acetonitrile/acetone mixture (v/v = 2/1) for 12 hours. Excess acetone was added to the slurry to ensure complete conversion of the PRX-HBA-ACT cocrystal. The slurry was then filtered to isolate the solids and the solids were allowed to dry.

Characterization

Optical Microscopy. Optical micrographs of crystals were taken with a Leica M205 C stereo microscope.

Raman Spectroscopy. On-chip Raman spectra was collected using a Renishaw mircoPL/Raman microscope equipped with a 785 nm excitation source and a Renishaw NIR 100 mW diode laser. Data was collected in the range of 600−1800 cm^{-1} at a spectral resolution of ~0.5 cm^{-1} at 1800 gratings/mm. Spectra were obtained over a 10 s exposure and averaged over 2 accumulations.

Single Crystal X-Ray Diffraction. Single crystal X-ray data was collected on a Bruker D8 Venture equipped with a four-circle kappa diffractometer and Photon 100 detector. An Iμs microfocus Cu source supplied the multi-mirror monochromated incident beam. A combination of Phi and Omega scans were used to collect the necessary data. A single crystal was picked and mounted on a 0.3mm loop using paratone oil. The PRX-HBA sample was cooled to 100 K or 222K (PRX-HBA or PRX-HBA-ACT, respectively) in a nitrogen supplied Oxford 700 Cryostream. Data was integrated using SAINT and absorption corrected using SAINT/SADABS v2012/1 or SAINT/SADABS v2014/2. The final structure was solved using SHELX-2013-4 or SHELX-2014-3.

Powder X-Ray Diffraction. Powder X-ray diffraction data was collected on a Rigaku Miniflex 600 in the Bragg-Brentano geometry. The data was collected from 3° – 80° 2θ with 0.02° steps and a 1.00 s detection time.

Thermogravimetric Analysis (TGA). Mass loss data was measured with a TA Q50. Approximately 10 mg of material was measured and placed in an alumina cup and loaded on a platinum pan. Samples

were heated from 25°C to 250°C at 5 °C /min. Dry nitrogen was used as a purge gas with a balance purge flow rate of 40 mL/min and sample purge flow rate of 60 mL/min.

Dynamic Scanning Calorimetry (DSC). Cocrystals thermograms were obtained using a TA Q2000. Approximately 5 mg of material was measured and crimped into a small aluminium pan. Samples were heated from 25 °C to 225 °C at 5 °C /min. An empty sealed aluminium pan was used as a reference. Dry nitrogen was used as a purge gas at a flow rate of 20 mL/min.

Results and Discussion

Platform Operation

The microfluidic platform is a 6 x 6 array of single wells, Figure 2. The platform layers and fabrication are as previously reported.[15, 22] Some details can be found in the Experimental section and Supplementary Information. The crystallization solution (1:1, 1:1.5 or 1:2 molar ratio of PRX and HBA) was stored in an Eppendorf tube off-chip and connected to the platform inlets via tubing. Solutions were introduced to the chambers on-chip upon actuation of the valve set by applying vacuum. While the valves were open, gentle suction at the corresponding fluidic outlets was applied. Once solutions were in the appropriate chambers, the valves were closed to isolate the chambers by removing vacuum. After the platform was filled, tape was placed over the fluidic inlets and outlets to prevent rapid solvent loss, and the platform was sealed in a Petri dish with Parafilm to further reduce solvent evaporation. Optical microscopy was used to identify crystals on-chip and Raman spectroscopy was used to determine the nature of the crystalline solids identified on-chip.

Cocrsytal Screen

Crystallization of PRX-HBA cocrystal was first carried out on-chip at 1:1 molar ratio in six solvents (mixtures), i.e. methanol, trifluoroethanol, acetonitrile, methanol/trifluoroethanol (v/v = 1/1), methanol/acetonitrile (v/v = 1/1), and trifluoroethanol/acetonitrile (v/v = 1/1). Thin needle-like crystals were observed in all solvents (mixtures) except in acetonitrile. The crystals collected in the three solvent mixtures were too small to give acceptable Raman scattering. Raman spectra of the needle-like crystals grown in methanol and trifluoroethanol was collected and found to matched with that of Form 18B1 previously reported by Childs et al..[10] Crystallization of PRX and HBA (**PRX-HBA**) in acetonitrile led to large prismatic crystals (Figure 3a) with an unique Raman spectra that has not been reported (Figure 3c).

On-chip crystallization of PRX and HBA was then repeated in acetonitrile with a molar ratio of 1:1.5

and 1:2, respectively, to determine the impact of HBA concentration on the solid form. At both conditions, crystals collected on-chip presented two different morphologies, i.e. prism and plate, with more plate-like crystals at higher HBA concentration. The Raman spectra of both crystals were collected on-chip. The plate-like crystals had the same Raman spectra as that of Form 18C as previously reported by Childs et al. (Figure 3c).[10] The prismatic crystals gave the same Raman spectra as the crystal identified in acetonitrile with PRX/HBA ratio of 1:1.

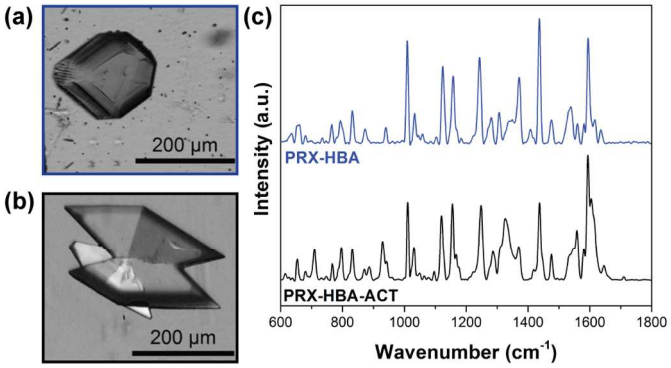

Figure 3. Images of (a) PRX-HBA and (b) PRX-HBA-ACT grown in acetonitrile and their corresponding (c) on-chip Raman spectra.

Structural Determination.

A crystal prepared in acetonitrile with molar ratio of PRX/HBA = 1:1 was removed from the platform and analyzed using single crystal x-ray diffractometer. The crystallographic information of its crystalline structure is shown in Table 1. The crystal was determined to be a PRX and HBA cocrystal (**PRX-HBA**) with a 1:1 molar ratio.

The plate-like crystals grown on-chip in acetonitrile with molar ratio of PRX/HBA = 1:1.5 were large enough for single crystal X-Ray diffraction. However they were found to be twinned (Figure 3b), which made the single-crystal diffraction data collection somewhat challenging. The first data collection was carried out at -200 °C. The diffraction data did not give a reliable structure solution, but suggested that the crystal had a triclinic unit cell. To facilitate single crystal data collection, crystallization was repeated off-chip with molar ratio of PXR/HBA = 1:1.5. A larger crystal with the same morphology (plate-like) was collected and tested using single crystal x-ray diffraction at -200 °C. The data suggested the same unit cell (triclinic) but again, did not give a reliable structure. Data collection was repeated after bringing the same crystal back to room temperature. The resulting unit cell and data quality remained the same. However, a fresh crystal with the plate-like morphology collected from the same preparation was found to have a monoclinic unit cell at room temperature without cooling to -200C initially. Following this observation, the x-ray diffraction of the monoclinic crystal was collected again

at -50C to reduce the thermal motion. A full data set was collected and the structure of the crystal was successfully solved (Table 1). The plate-like crystal was found to be an acetone solvate of PRX-HBA cocrystal with a molar ratio of 1:1:1 (**PRX-HBA-ACT**), Figure 4. This finding came as a surprise because acetone was not used in crystallization. We believe acetone was introduced with HBA as an impurity. This may be an excellent example on the impact of trace amount of impurity on the result of crystallization.

To confirm the source of acetone further experiments were performed. Repeating the previously mentioned experiments using a different batch of acetonitrile yielded the same outcome, namely that the PRX-HBA-ACT cocrystal was observed in the experiments with a molar ratio of PRX/HBA = 1:1.5 and 1:2. Since the acetone was believed to be present in the HBA, we heat-treated the HBA at 100 °C for 3 hours, presumably removing any remaining acetone. When repeating the crystallization experiments using this heat-treated HBA, only PRX:HBA cocrystals were obtained, strongly suggesting that the acetone indeed was an impurity in the HBA.

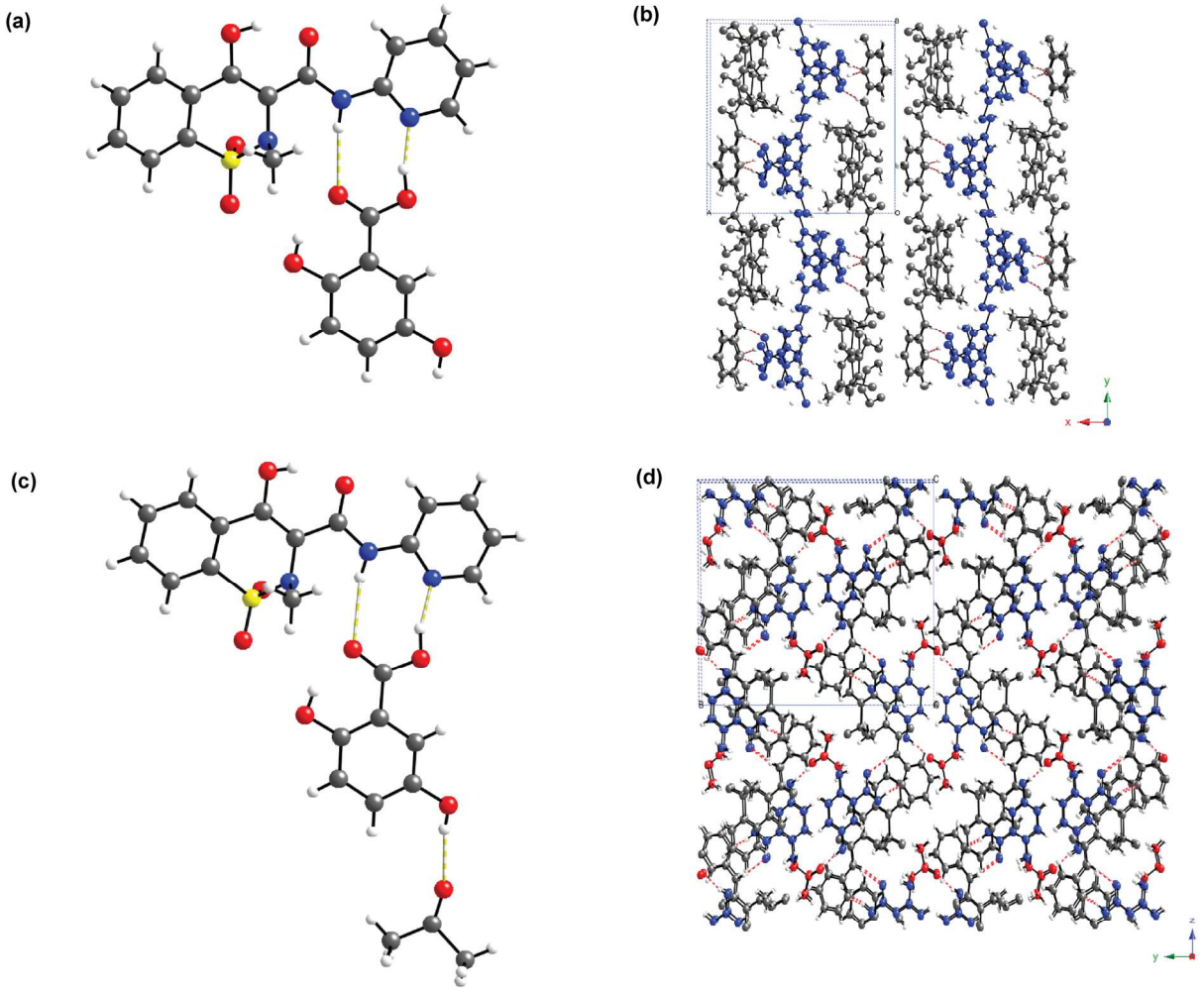

Figure 4. (a) Asymmetric unit of PRX-HBA. (b) Several unit cells of the PRX-HBA crystal structure

looking down the a-axis highlighting the wavy 1-D chains formed (PRX (grey) HBA (blue)). (c) Asymmetric unit of PRX-HBA-ACT. (d) Several unit cells of the PRX-HBA-ACT crystal structure looking down the c-axis showing the position of the acetone molecules in the crystal structure (PRX (grey) HBA (blue) ACT (red)).

Table 1. Crystallographic information for PRX-HBA and PRX-HBA-ACT

	PRX-HBA	PRX-HBA-ACT
chemical formula	$C_{15}H_{13}N_3O_4S$, $C_7H_6O_4$	$C_{15}H_{13}N_3O_4S$, $C_7H_6O_4$, C_3H_6O
formula weight	485.47	543.54
T (K)	100	222
crystal system	monoclinic	monoclinic
space group	$P2_1/c$	$P2_1/c$
***a* (Å)**	14.243	6.839
***b* (Å)**	13.561	22.396
***c* (Å)**	11.714	16.322
α (deg)	90.00	90.00
β (deg)	112.52	98.71
γ (deg)	90.00	90.00
volume (A^3)	2090.02	2471.27
D_{calcd} (g cm^{-3})	1.543	1.461
Z	4	4
data/ restraints/ parameters	3777/ 0/ 323	4419/ 150/ 400
R_1	0.0357	0.0662
wR_2	0.0869	0.1721
GOF	1.022	1.195
Completeness	98.6	97.2
Color	colorless	colorless

Crystal Structure Analysis

PRX-HBA crystallizes in the monoclinic space group $P2_1/c$ with one PRX and one HBA molecule in the asymmetric unit. Hydrogen bonding occurs between the pyridine and amide nitrogen atoms of PRX and the carboxylic acid of HBA. The hydroxy substituent in the 5- position on the HBA in the PRX:HBA cocrystal is hydrogen bonded to the hydroxyl substituent in the 2-position of a neighboring HBA. All hydrogen bonding occurs in one plane creating a 1-D wavy structure (Figure 4b). PRX-HBA-ACT also crystallizes in the monoclinic space group $P2_1/c$ with one PRX, HBA, and ACT molecule in the asymmetric unit. Hydrogen bonding occurs between the pyridine and amide nitrogen

atoms of PRX and the carboxylic acid of HBA. The hydroxyl on the 5 position on the HBA is hydrogen bonded to the carbonyl oxygen in ACT. The ACT molecules are arranged along the a-axis, which is evident when looking at a stack of several unit cells of this crystal structure along this axis (Figure 4d). This arrangement possibly allows the ACT molecules to escape from the crystal structure when heated (experiment described below) without interrupting the hydrogen bonding between PRX and HBA.

Thermal Characterization

A slurry method (see Experimental section) was used to obtain gram-scale quantities of PRX-HBA and PRX-HBA-ACT for thermal characterization. Raman spectroscopy was used to confirm the identity the slurried products.

Thermogravimetric Analysis (TGA). Thermogravimetric analysis was used to determine the temperature at which significant weight loss is observed, Figure 5. Heated at 5 °C/min, solids of the starting materials PRX and HBA, and of the PRX-HBA cocrystal remained thermally stable until 200 °C, at which temperature the solids degraded. No mass loss was detectable due to acetone desolvation from the HBA, possibly due to detection limits of the instrument. The solid of PRX-HBA-ACT lost ~10.4% of its weight at 80 °C, presumably due to the loss of acetone from its lattice. This mass loss is in close agreement with the theoretical value of 10.7%. The solid degraded at 200 °C when heated further.

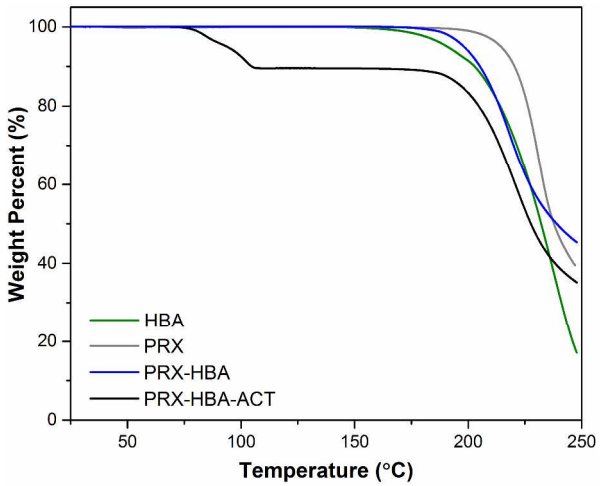

Figure 5. Thermogravametric analysis data showing a 10.4% mass loss in PRX-HBA-ACT from desolvation of acetone beginning at 80 °C. There is no noticeable mass loss in PRX, HBA, or PRX-HBA.

Powder X-ray Diffraction (PXRD). PRX-HBA-ACT solids were held at three temperatures to evaluate the physical stability of the solid form, Figure 6. The solids were stored at room temperature (~

25 °C), 65 °C, and 100 °C for up to 1 month, 1 day, and 1 hour, respectively. After being exposed to the variety of temperatures the solids were cooled to room temperature and PXRD data was collected. The PXRD patterns of the PRX-HBA-ACT solid remained unchanged after being held at room temperature for 1 month. When were stored at 65 °C, the solid remained primarily unchanged in 1 hour with slight peak shifts to the right and an extra diffraction peak appearing at about 24° 2θ. These changes became more prominent after storage for 1 day at 65 °C. The resulting PXRD pattern now resembles the PRX-HBA spectra with slight peak shifts to the right. The solid stored at 100 °C for 1 hour closely resembles the peak shapes and intensities of the 1 day at 65 °C data but the peak positions correspond exactly to

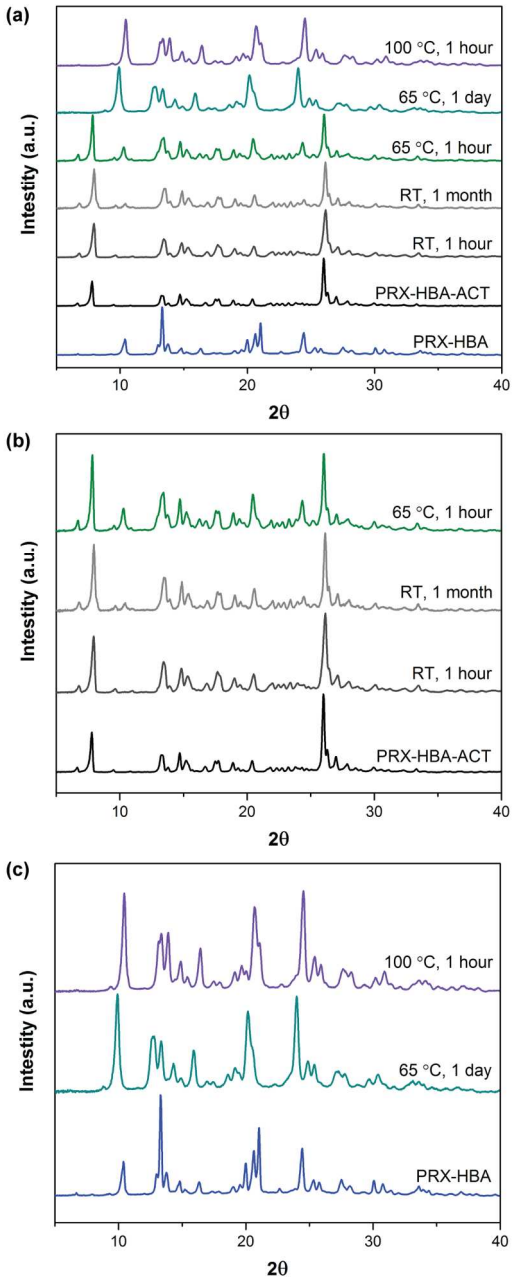

Figure 6. (a) Powder X-ray diffraction data from a thermal stability study of PRX-HBA-ACT. (b) Comparisons of powder patterns from PRX-HBA-ACT that were heat treated at 25 °C for 1 hour and 1 month, and 65 °C for 1 hour which closely resembles the initial PRX-HBA-ACT powder pattern. (c) Powder patterns of PRX-HBA-ACT that were heat treated at 65 °C for 1 day and 100 °C for 1 hour compared to PRX-HBA powder patterns. As PRX-HBA-ACT loses ACT, the powder patterns begin to resemble that of PRX-HBA.

the peak positions observed for PRX-HBA. The heated samples show slightly broader peaks when compared to PRX-HBA indicating that the heated samples have a smaller crystal size. Additionally, peak intensities of the heated samples do not directly correspond to the PRX-HBA, possibly due to preferred orientation of the heated samples. Comparison of these patterns with those of the non-solvated cocrystal PRX-HBA, suggests that the solid of PRX-HBA-ACT converts to the non-solvated cocrystal at elevated temperature and that the extent of conversion is temperature dependent.

Differential Scanning Calorimetry (DSC). The thermal events of the cocrystals and each of their components were recorded while heated to 250 °C. Solids of PRX-HBA exhibited a sharp melting endotherm at 194 °C followed by a weaker endothermic peak at 202 °C. We tentatively attribute these peaks to sublimation of HBA, which shows peaks at 202 °C and 206 °C, or melting of PRX, 201 °C, that partially crystallized after melting of the cocrystal. Solids of PRX-HBA-ACT showed a broad endothermic peak at beginning at 65 °C and continuing to 104 °C likely due to desolvation of the cocrystal. The desolvated cocrystal melts at 194 °C followed by a weaker endothermic peak at 202 °C. The two cocrystals had the same melting temperatures and profiles suggesting that the solvate may have partially converted to the non-solvated cocrystal upon heating.

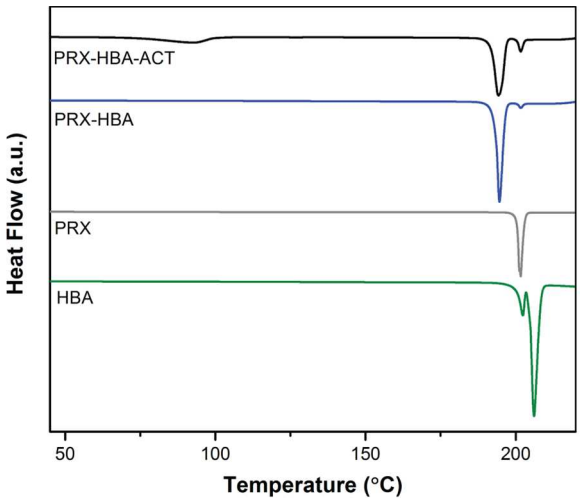

Figure 7. Differential scanning calorimeter data for PRX, HBA, PRX-HBA, and PRX-HBA-ACT. A small bump in the graph can be seen in the PRX-HBA-ACT graph near 105 °C from the desolvation of acetone. Both cocrystals have a lower melting point than the melting point of PRX and the sublimation temperature of HBA.

Conclusions

In this work, a cocrystal screen of PRX and HBA was used as a model system to investigate cocrystalliztion of BCS Class II compounds. Class II compounds make up the majority of the drugs currently in the pharmaceutical pipeline and increasing the solubility of the API, for example via cocrystallization, could ultimately determine the fate of the API. We developed a simple microfluidic platform to perform a cocrystal screen by solution mediated phase transformation through solvent evaporation. The platform is comprised of a 6x6 array of single wells that are isolated with normally closed valves to replicate the experimental conditions of a 96 well plate. The shallow wells (~60 μm) and transparent chip materials allow for easy detection of solid forms on-chip as well as subsequent characterization of these solid forms with Raman spectroscopy. The platform is easy to manufacture and operate and only requires a vacuum source for filling.

We have prepared and characterized a PRX-HBA cocrystal and a PRX-HBA-ACT solvated cocrystal. We were surprised to find acetone incorporated into the crystal structure of this second solid form, since no acetone was added to the crystallization solution. We synthesized bulk quantities of both cocrystals for physical characterization *via* TGA, PXRD, and DSC. With TGA we only observed noticeable mass loss from PRX-HBA-ACT, 10.4 wt%, attributed to desolvation of acetone. Investigation of the stability of PRX-HBA-ACT revealed that this solid form is stable at 25 °C and 65 °C for a short period of time. Upon increasing the temperature to 100 °C or upon holding at 65 °C for a day, the PRX-HBA-ACT desolvated resulting in a powder diffraction pattern that is similar to the powder diffraction pattern obtained for PRX-HBA. In this work we demonstrated the utility of microfluidics in pharmaceutical drug discovery, in particular with respect to solid form screening and subsequent solid form characterization. The results presented here also underscore the importance of crystal structure determination to confirm solid form.

Acknowledgements

We would like to thank AbbVie Inc. for financial support and the National Science Foundation for a Graduate Research Fellowship to EMH (Grant DGE-1144245). We would like to acknowledge Dr. Danielle Gray for help collecting and solving the single crystal diffraction data. Part of this work was carried out in the George L. Clark X-ray Facility and 3M Materials Laboratory, Micro- & Nanotechnology Laboratory, and the Frederick Seitz Materials Research Laboratory at the University of Illinois at Urbana-Champaign.

Notes and references

[a] *Department of Chemical & Biomolecular Engineering, University of Illinois at Urbana-Champaign, 600 South Mathews Avenue, Urbana, Illinois 61801,USA.*
[b] *School of Chemical Sciences, University of Illinois at Urbana-Champaign, 505 South Mathews Avenue, Urbana, Illinois 61801,USA.*
[c] *Drug Product Development, Research and Development, AbbVie Inc., 1 North Waukegan Road, North Chicago, Illinois 60064, USA.*

*Paul J.A. Kenis
Phone: (217) 265-0523
Fax: (217) 333-5052
Email: kenis@illinois.edu
Web Address: http://www.scs.uiuc.edu/~pkgroup/

*Yuchuan Gong
Phone: (847) 938-6642
Fax: (847) 937-2417
Email: yuchuan.gong@abbvie.com

† The University of Illinois at Urbana, Champaign and AbbVie jointly participated in study design, research, data collection, analysis and interpretation of data, writing, reviewing, and approving the publication. Geoff G. Z. Zhang and Yuchuan Gong may own AbbVie stock. Information about microfluidic platform manufacturing can be found in the Supplemental Information.

1. **G. L. Amidon, H. Lennernas, V. P. Shah and J. R. Crison, *Pharmaceutical Research*, 1995, 12, 413-420.**

2. **A. M. Thayer, *Chemical & Engineering News Archive*, 2010, 88, 13-18.**

3. **A. M. Chen, M. E. Ellison, A. Peresypkin, R. M. Wenslow, N. Variankaval, C. G. Savarin, T. K. Natishan, D. J. Mathre, P. G. Dormer, D. H. Euler, R. G. Ball, Z. Ye, Y. Wang and I. Santos, *Chemical Communications*, 2007, 419-421.**

4. **S. L. Childs, L. J. Chyall, J. T. Dunlap, V. N. Smolenskaya, B. C. Stahly and G. P. Stahly, *Journal of the American Chemical Society*, 2004, 126, 13335-13342.**

5. **J. F. Remenar, S. L. Morissette, M. L. Peterson, B. Moulton, J. M. MacPhee, H. R. Guzmán and Ö. Almarsson, *Journal of the American Chemical Society*, 2003, 125, 8456-8457.**

6. **A. V. Trask, W. D. Samuel Motherwell and W. Jones, *Crystal Growth and Design*, 2005, 5, 1013-1021.**

7. **S. J. Nehm, B. Rodríguez-Spong and N. Rodríguez-Hornedo, *Crystal Growth and Design*, 2006, 6, 592-600.**

8. **A. V. Trask, W. D. S. Motherwell and W. Jones, *International Journal of Pharmaceutics*, 2006, 320, 114-123.**

9. **N. J. Babu and A. Nangia, *Crystal Growth and Design*, 2011, 11, 2662-2679.**

10. **S. L. Childs and K. I. Hardcastle, *Crystal Growth and Design*, 2007, 7, 1291-1304.**

11. **D. K. Bučar, R. F. Henry, X. Lou, R. W. Duerst, L. R. MacGillivray and G. G. Z. Zhang, *Crystal Growth and Design*, 2009, 9, 1932-1943.**

12. **J. R. G. Sander, D. K. Bučar, R. F. Henry, B. N. Giangiorgi, G. G. Z. Zhang and L. R. MacGillivray, *CrystEngComm*, 2013, 15, 4816-4822.**

13. **C. R. Groom and F. H. Allen, *Angewandte Chemie - International Edition*, 2014, 53, 662-671.**

14. **A. Bak, A. Gore, E. Yanez, M. Stanton, S. Tufekcic, R. Syed, A. Akrami, M. Rose, S. Surapaneni, T. Bostick, A. King, S. Neervannan, D. Ostovic and A. Koparkar, *Journal of Pharmaceutical Sciences*, 2008, 97, 3942-3956.**

15. **S. Goyal, M. R. Thorson, C. L. Schneider, G. G. Z. Zhang, Y. Gong and P. J. A. Kenis, *Lab on a Chip - Miniaturisation for Chemistry and Biology*, 2013, 13, 1708-1723.**

16. **M. R. Thorson, S. Goyal, Y. Gong, G. G. Z. Zhang and P. J. A. Kenis, *CrystEngComm*, 2012, 14, 2404-2412.**

17. **M. R. Thorson, S. Goyal, B. R. Schudel, C. F. Zukoski, G. G. Z. Zhang, Y. Gong and P. J. A. Kenis, *Lab on a Chip - Miniaturisation for Chemistry and Biology*, 2011, 11, 3829-3837.**

18. **R. A. L. Leon, W. Y. Wan, A. Z. M. Badruddoza, T. A. Hatton and S. A. Khan, *Crystal Growth and Design*, 2014, 14, 140-146.**

19. **P. A. Anquetil, C. J. H. Brenan, C. Marcolli and I. W. Hunter, *Journal of Pharmaceutical Sciences*, 2003, 92, 149-160.**

20. **D. Lombardi and P. S. Dittrich, *Expert Opinion on Drug Discovery*, 2010, 5, 1081-1094.**

21. **J. Puigmarti-Luis, *Chemical Society Reviews*, 2014, 43, 2253-2271.**

22. **S. Goyal, M. R. Thorson, G. G. Z. Zhang, Y. Gong and P. J. A. Kenis, *Crystal Growth and Design*, 2012, 12, 6023-6034.**

TOC

*****For use in the table of contents only*****

Two cocrystals of piroxicam (PRX) and 2,5-dihydroxybenzoic acid (HBA) were found using a microfluidic cocrystal screening approach; one crystal contained an acetone (ACT) impurity.